AD A137258

ADF300372

MEMORANDUM REPORT ARBRL-MR-03330

CHARACTERIZATION OF FLOW INTERACTION OF A WATER JET WITH A CHEMICAL CONTAMINANT DROPLET

Lang-Mann Chang

December 1983

US ARMY ARMAMENT RESEARCH AND DEVELOPMENT CENTER
BALLISTIC RESEARCH LABORATORY
ABERDEEN PROVING GROUND, MARYLAND

Approved for public release; distribution unlimited.

Additional copies of this report may be obtained from the National Technical Information Service, U. S. Department of Commerce, Springfield, Virginia 22161.

UNCLASSIFIED

SECURITY CLASSIFICATION OF THIS PAGE (When Data Entered)

REPORT DOCUMENTATION PAGE

READ INSTRUCTIONS BEFORE COMPLETING FORM

1. REPORT NUMBER
MEMORANDUM REPORT ARBRL-MR-03330

2. GOVT ACCESSION NO.
AD-A137 257

3. RECIPIENT'S CATALOG NUMBER

4. TITLE (and Subtitle)
CHARACTERIZATION OF FLOW INTERACTION OF A WATER JET WITH A CHEMICAL CONTAMINANT DROPLET

5. TYPE OF REPORT & PERIOD COVERED

6. PERFORMING ORG. REPORT NUMBER

7. AUTHOR(s)
Lang-Mann Chang

8. CONTRACT OR GRANT NUMBER(s)

9. PERFORMING ORGANIZATION NAME AND ADDRESS
US Army Ballistic Research Laboratory, ARDC
ATTN: DRDAR-BLI (A)
Aberdeen Proving Ground, Maryland 21005

10. PROGRAM ELEMENT, PROJECT, TASK AREA & WORK UNIT NUMBERS
1L161102A71A

11. CONTROLLING OFFICE NAME AND ADDRESS
US Army AMCCOM, ARDC
Ballistic Research Laboratory, ATTN: DRSMC-BLA-S(A)
Aberdeen Proving Ground, Maryland 21005

12. REPORT DATE
December 1983

13. NUMBER OF PAGES
20

14. MONITORING AGENCY NAME & ADDRESS(if different from Controlling Office)

15. SECURITY CLASS. (of this report)
UNCLASSIFIED

15a. DECLASSIFICATION/DOWNGRADING SCHEDULE

16. DISTRIBUTION STATEMENT (of this Report)

Approved for public release; distribution unlimited.

17. DISTRIBUTION STATEMENT (of the abstract entered in Block 20, if different from Report)

18. SUPPLEMENTARY NOTES

19. KEY WORDS (Continue on reverse side if necessary and identify by block number)

Chemical Decontamination
Contaminant Droplet
Flow Parameters
Water Jet Impingement
Jet-Droplet Interaction Flow

20. ABSTRACT (Continue on reverse side if necessary and identify by block number) ker

Two flow models are developed for the study of the interaction of a water jet with a chemical contaminant droplet on a flat surface which occurs in chemical decontamination processes. The interaction flow is considered as a two-dimensional viscous flow. Computer-generated plots are presented to show the flow pattern and the evolution of the contaminant droplet with various viscosities. The effects of the jet incidence angle and the jet (Continued on reverse side)

DD FORM 1473 1 JAN 73 EDITION OF 1 NOV 65 IS OBSOLETE

UNCLASSIFIED

SECURITY CLASSIFICATION OF THIS PAGE (When Data Entered)

20. ABSTRACT (Continued)

velocity on the movement of the droplet are described. The computed result shows that the instantaneous impact pressure peak on the contaminated surface can rise much higher than the corresponding steady-state dynamic pressure of the jet.

TABLE OF CONTENTS

LIST OF FIGURES

I. INTRODUCTION

Of various methods proposed for removal of the contaminant droplets on surfaces of a vehicle or other equipment, utilization of water jets appears to be the most effective and the most economical one at the current level of technological development. The procedure is to use the water jet to break up the droplet and subsequently to carry away the contaminant. The surfaces then can be decontaminated by moving an assemblage of water jets toward the contaminant droplets.

In order to design an efficient jet system, the following knowledge is vital: the general flow pattern, the evolution of the contaminant droplet, and the effect of each flow parameter on the flow. This information can be sought via experiments, but that would require very sophisticated instrumentation and would be very costly. As an alternative, one may use computer simulations based on appropriate flow models. In fact, this method can have a much greater flexibility than experiments for examining areas of importance in the flow field and, therefore, can provide better insights into the flow phenomena.

The jet-droplet interaction is a three-dimensional, transient, two-fluid flow. The flow is extremely complicated since it involves interfaces separating the two fluids and each of the fluids may have free surfaces with the ambient. In the present investigation, we have simplified the problem by treating it as a two-dimensional flow for which we have developed two flow models, namely, one-fluid flow and two-fluid flow. They are suitable for the computation of the development of two different pre-impingement flow configurations. Results presented are the flow pattern, evolution of a contaminant droplet, effects of variation of flow parameters on the flow, and some typical pressure distributions on the impingement surface.

II. FLOW MODELS

Figure 1 depicts two pre-impingement flow situations which can occur in the decontamination process. In the first configuration, shown in Figure 1a, a water jet is directed at a contaminant droplet which is covered by a water layer. The water layer is stationary or flowing. In the second configuration, shown in Figure 1b, there is no water coverage on the contaminant droplet. To respectively characterize the flows developing from the two configurations we have developed a two-fluid flow model and a one-fluid flow model. Both models describe a two-dimensional viscous flow and can be handled by the computer code SOLA-VOF (Reference 1). It is noted that the computer code can solve flow problems involving fluids separated by interfaces in a region without voids or one fluid with voids (ambient).

---

[1] *B.D. Nicholas, C.W. Hirt, and R.S. Hotchkiss, "SOLA-VOF: A Solution Algorithm for Transient Fluid Flow with Multiple Free Boundaries," Los Alamos Scientific Laboratory Report No. LA-8355, 1980.*

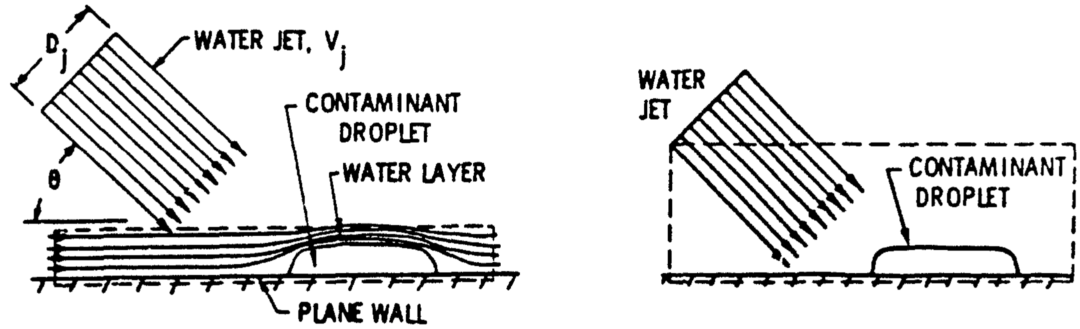

a. Contaminant Droplet with Initial Water Layer Coverage (Two-Fluid Flow)

b. Contaminant Droplet Without Initial Water Layer Coverage (One-Fluid Flow)

Figure 1. Pre-Impingement Flow Configuration

A. Two-Fluid Flow Model

This is a model of a channel-type flow bounded by the dashed line indicated in Figure 1a, covering the major part of the flow region. The channel contains two fluids (water and contaminant) separated by an interface. The upper wall of the channel coincides with the upper free surface of the water layer so as to eliminate consideration of the free surface with the ambient. An outflow boundary condition is specified at this wall and at the ends of the channel, allowing the fluids to flow out the region. The contaminant which covers a rectangular region is assumed to wet perfectly the lower wall of the channel. To account for viscous effects, a no-slip condition is used at the lower wall. Finally, a steady uniform jet velocity is specified along a segment of the upper wall as shown on the top of Figure 2.

B. One-Fluid Flow Model

Results of computations with the two-fluid flow model show that for such a close-in impingement the interaction flow is insensitive to the variation of viscosity of the jet fluid. Also, the density of the contaminant (1070 kg/m^3) is very close to that of plain water (1000 kg/m^3). Therefore, we can simplify the problem by setting the physical properties of the jet fluid (water) equal to that of the contaminant and treat the jet-droplet flow as a one-fluid flow. The flow region for computation is bounded by the dashed line in Figure 1b. In this model, only the free surface with the ambient is traced, but not the interface between the water and the droplet. The one-fluid flow model is suitable for characterizing the flow developing from the configuration of Figure 1b for which the two-fluid flow model is beyond the capability of the SOLA-VOF code because the model requires the tracing of two surfaces, i.e., the interface and the free surface.

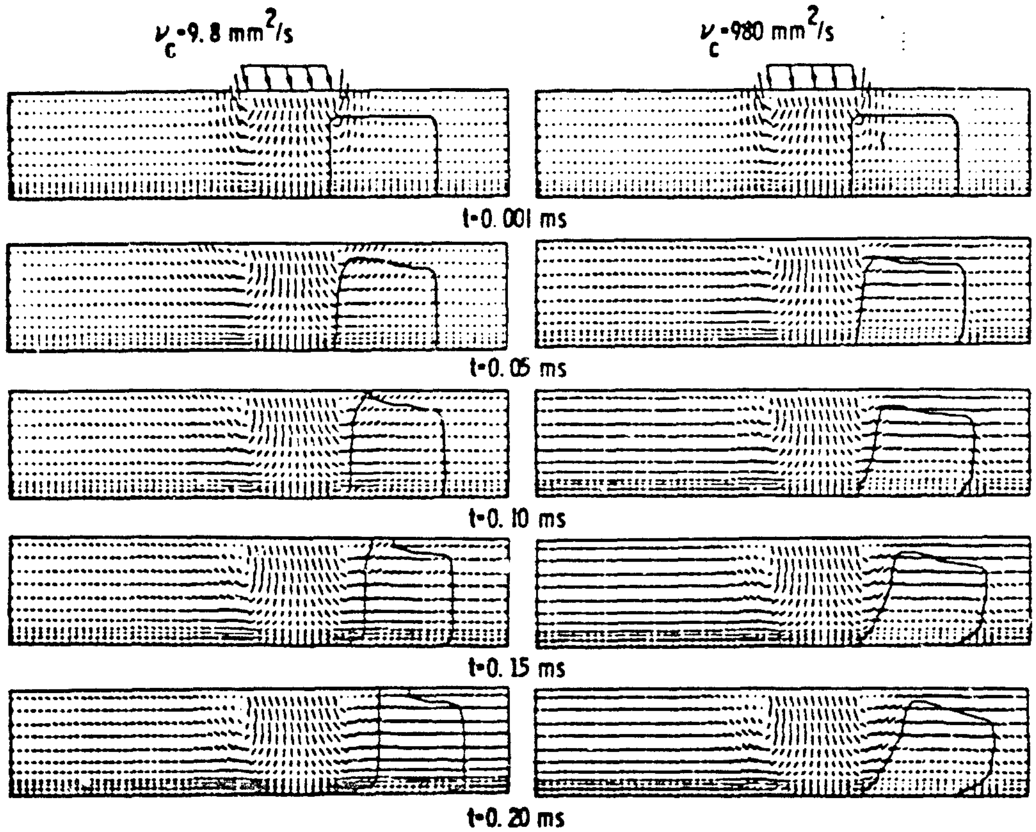

Figure 2. Flow Patterns (Two-Fluid Flow, $\nu_w = 0.98\ mm^2/s$, $V_j = 5\ m/s$, $\theta = 45°$)

III. BASIC GOVERNING EQUATIONS AND COMPUTATIONAL RESULTS

The basic equations governing the flow are the two-dimensional, unsteady, incompressible Navier-Stokes equations and the continuity equation. They are solved in the SOLA-VOF code by using a finite difference scheme. The free surface (or interface) is defined by a function F which satisfies the equation

$$\frac{\partial F}{\partial t} + u\frac{\partial F}{\partial x} + v\frac{\partial F}{\partial y} = 0 \quad (1)$$

where u and v are the velocity components in x and y directions, respectively. This equation states that F moves with the fluid. The value of F is unity in computing cells fully occupied by a fluid and is zero in cells without such a fluid. Cells with F values between zero and one contain free surfaces. Using this technique, the free surface can be tracked by monitoring the values of

F. In addition, the code allows one to embed Marker Particles in the region covered by the contaminant droplet, providing a good visualization of the evolution of the droplet.

The dimensions of the droplet for computation were assumed to be 3 mm x 0.6 mm (length by height), representing the average size of the droplet on a flat surface. Other input data were:

D_j = jet size = 1.83 mm

V_j = jet velocity = 5 - 10 m/s, corresponding to steady dynamic pressure of 14 - 50 kPa (2 - 7.2 psi) which are practical for decontamination

ρ_c = contaminant density = 1070 kg/m^3, for water ρ_w = 1000 kg/m^3

ν_c = kinematic viscosity of contaminant = 9.8 - 980 mm^2/s, equivalent to 10 - 1000 times the kinematic viscosity of water ν_w

A. Two-Fluid Flow Model (Contaminant Droplet with Initial Water Layer Coverage)

Figure 2 shows the computational domain of the flow field, which has a dimension of 20 mm x 0.8 mm. The rectangle in the flow channel is the region initally covered by the contaminant droplet. The velocity and the incidence angle of the jet are, respectively, V_j = 5 m/s and θ = 45°. It is noted that all of the graphs in this figure have been magnified by a factor of 3 in the vertical direction in order to give a better visualization of the flow near the bottom surface of the channel where a finer computational mesh was used. The vectors represent the local velocities in the individual cells of the mesh. The figure shows the flow development following the commencement of the jet impingement up to 0.2 millisecond. The results for two contaminant viscosities, ν_c = 9.8 mm^2/s and ν_c = 980 mm^2/s, are shown in the left and the right columns, respectively. Figure 3 provides another view of evolution of the droplet.

The viscosity has a pronounced effect as shown by the droplet profiles and the displacements, S, of the droplet upstream edge. In addition, the fluid particles in the low viscosity droplet have been disturbed in the entire region, while in the high viscosity droplet there still exists a region near the surface in which the fluid particles remain in good order. This is an indication that the two droplets are subjected to different stress levels.

The displacement S shown in Figure 3 is defined as the distance from the initial location of the upstream edge of the droplet (marked by the dashed line) to the nearest marker particle of the droplet region on the first row above the impingement surface. We embedded 24 rows of marker particles uniformly across the droplet in the vertical direction and there were 30 marker particles in each row. As illustrated in Figure 4, the nearest marker particle from the dashed line is not always the one which orginally resided at the very left end of the first row. This is because the jet stream is lifted off the impingement surface and the marker particles in the front are carried

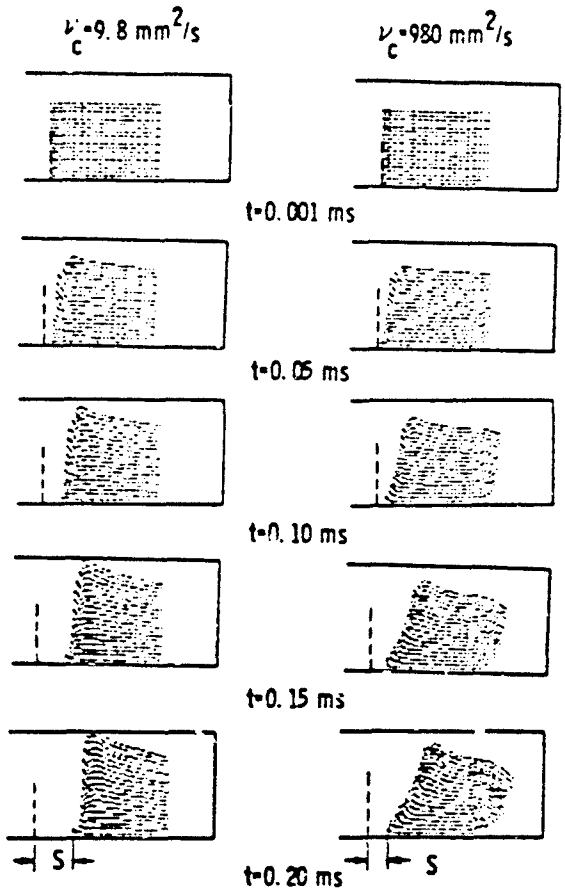

Figure 3. Evolution of Contaminant Droplets
(ν_w = 0.98 mm^2/s, V_j = 5 m/s, θ = 45°)

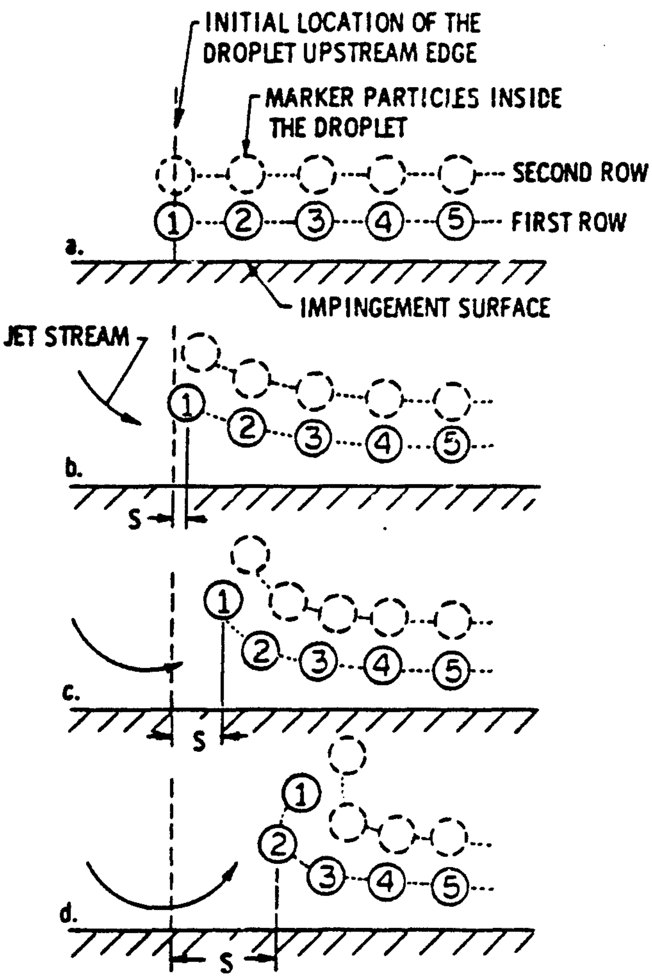

Figure 4. Movements of Marker Particles Following the Start of the Jet Flow (Definition of the Displacement S)

upward. The location of each marker particle following the jet impingement can be traced and printed out by the computer. The displacement S defined, in fact, is dependent on the number of rows of marker particles embedded and the the fineness of the computational mesh size used. A larger number of rows and a finer mesh size will certainly result in a smaller displacement S. In the present study, due to the excessive costs of computer time and the problems of numerical instability and divergence encountered, the finest cell size in the vertical direction used near the impingement surface after 0.025 mm, which is approximately 4% of the droplet height. The initial distance between the first row of marker particles and the impingement surface was also 0.025 mm. Test runs using different mesh sizes show no significant changes in the droplet profile except in the thin layer very close to the impingement surface.

Figure 5 shows the effect of the jet incidence angle θ on the displacement S. A jet at a smaller incidence angle has a larger portion of the jet stream moving toward the droplet; however, it produces less normal force to displace the droplet because of a smaller rate change of momentum in the impingement area. A jet at a larger incidence angle has the opposite result. Therefore, there is an optimum angle at which a jet produces the largest displacement S. For the case that $\upsilon_c = 9.8$ mm^2/s and $V_j = 5$ m/s and that the jet is fixed in a location where the largest S can be obtained, we have found that a jet at $\theta = 45 - 60°$ gives the best performance. Further investigations are in progress for cases with other viscosities and jet velocities.

B. One-Fluid Flow Model (Contaminant Droplet without Initial Water Layer Coverage)

We next consider the flow configuration of Figure 1b which is treated by the one-fluid flow model. Figure 6 shows a sequence of flow development following the initiation of the impingement. The jet stream first spreads out on the wall, then engages the droplet and finally is lifted off the wall at some angle. The figures shows free surfaces with the ambient, but no interfaces between the jet fluid and the droplet because the latter interfaces are not traced by the one-fluid flow model. However, the evolution of the droplet can be visualized by the movement of the marker particles shown in Figure 7. A comparison of the columns in Figure 7 shows the flow dependence on the viscosity.

Figure 8 is a plot of the mean velocity $\dot{S}$ of the droplet upstream edge versus the displacement S of the droplet upstream edge, where $\dot{S} = S/t$ and t is the time for the displacement reaching to S after the start of the jet flow. The jet velocity strongly affects the mean velocity $\dot{S}$ of the droplet. If the viscosity $\upsilon_c = \upsilon_w = 98$ mm^2/s, then for $V_j > 5$ m/s the droplet upstream edge can move with a velocity greater than 3 m/s at its early movement, say, in the first 0.4 mm of displacement. The velocity is large enough to displace the droplet practically instantaneously at the impingement.

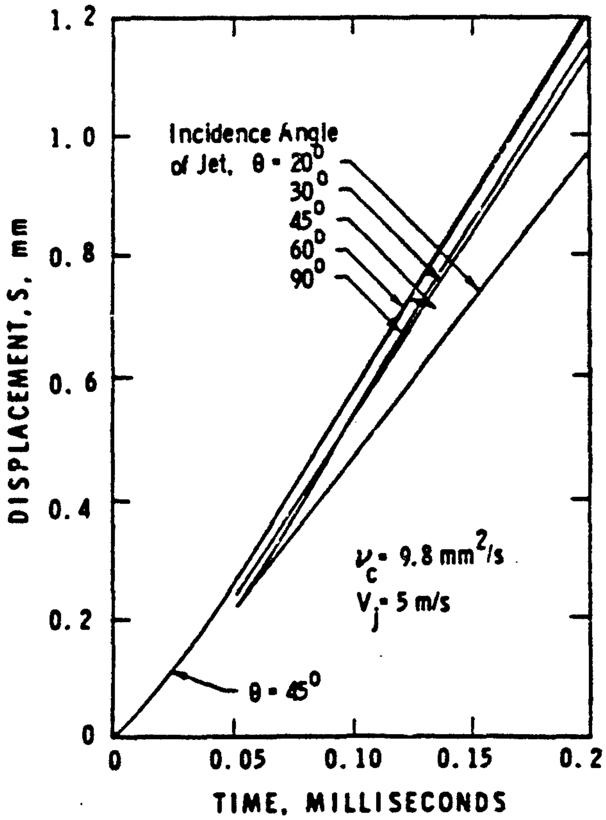

Figure 5. Displacement of Contaminant Droplet Upstream Edge vs. Time After Commencement of Jet Flow

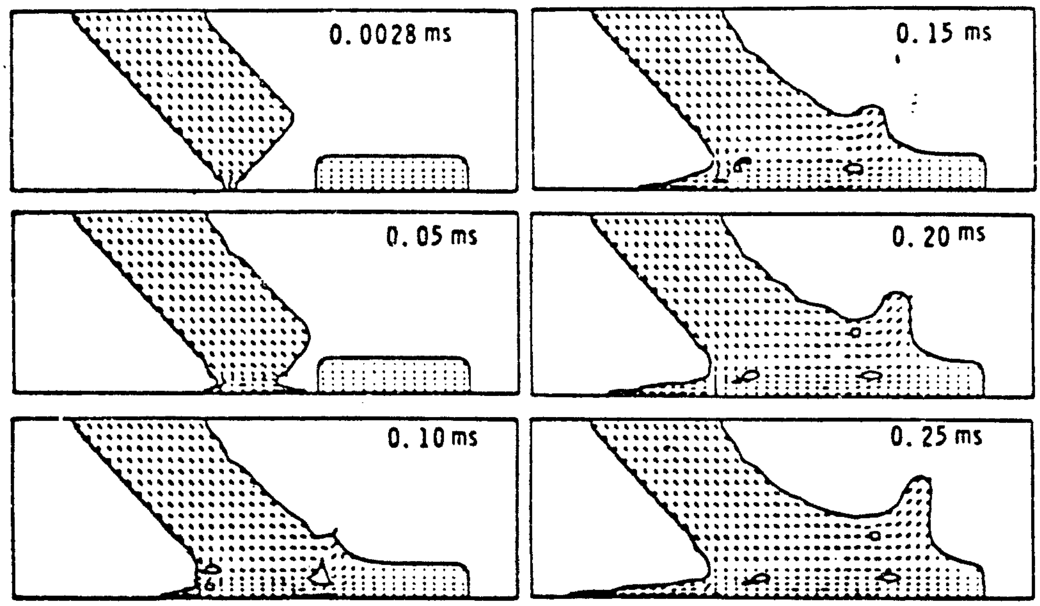

Figure 6. Flow Pattern (One-Fluid Flow, $\nu_c = \nu_w = 9.8\ mm^2/s$, $V_j = 10\ m/s$, $\theta = 45°$)

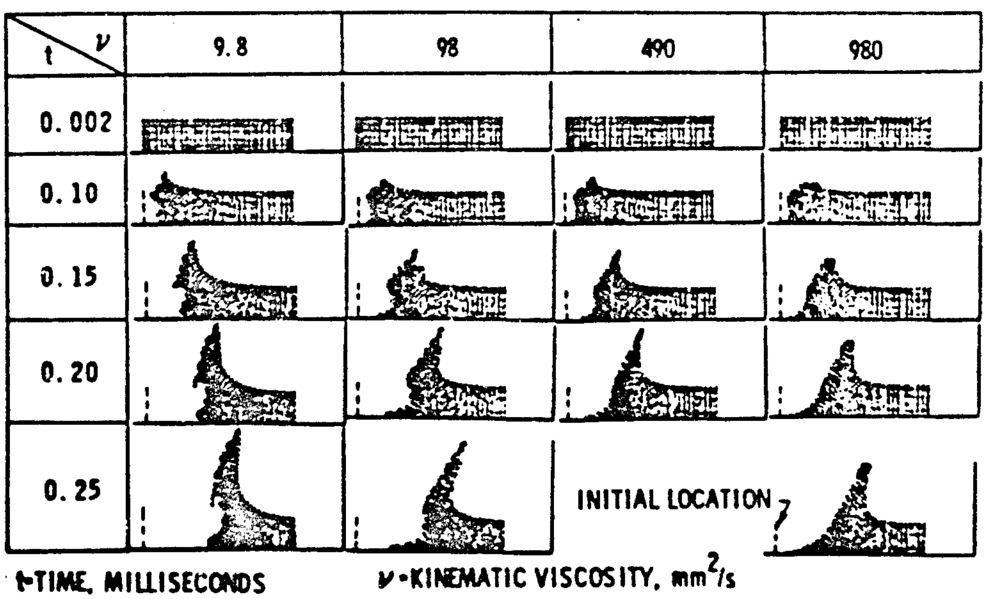

Figure 7. Evolution of Contaminant Droplets (One-Fluid Flow, $V_j = 10\ m/s$, $\theta = 45°$)

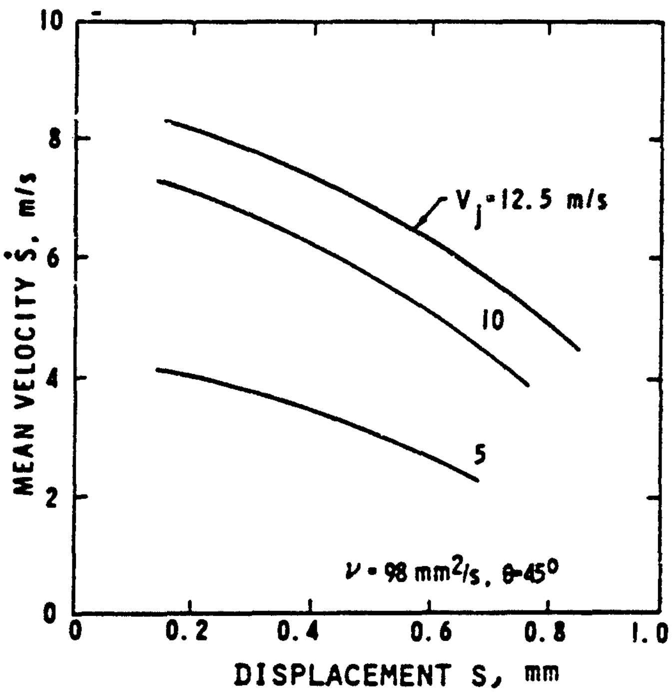

Figure 8. Mean Velocity of Droplet Upstream Edge, $\dot{S}$, vs. Displacement of Droplet Upstream Edge, S

Figures 9 and 10 present a comparison of flows corresponding to two jet sizes, $D_j = D$ and $D_j = 2.5$ D, for the jet incidence angle $\theta = 0°$. We see that the additional amount of the jet fluid does not increase significantly the displacement of the lower part of the droplet but simply flows over it. Investigations for cases with $\theta > 0°$ are currently underway. Based on the above results, however, we can expect that for a limited jet flow rate, increasing the jet velocity rather than the jet size will give a better performance in decontamination.

Another area of concern is the rise of the pressure peak on the impingment surface. In some critical areas, such as the optical windows of a vehicle, the impact pressure that the areas can withstand is limited. Figure 11 presents some typical pressure distributions on the impingement surface after the start of the jet flow. Because the phenomenon is transient, the instantaneous pressure peaks can rise higher than twice the corresponding steady dynamic pressure of the jet velocity, $1/2\ (\rho V_j^2)$.

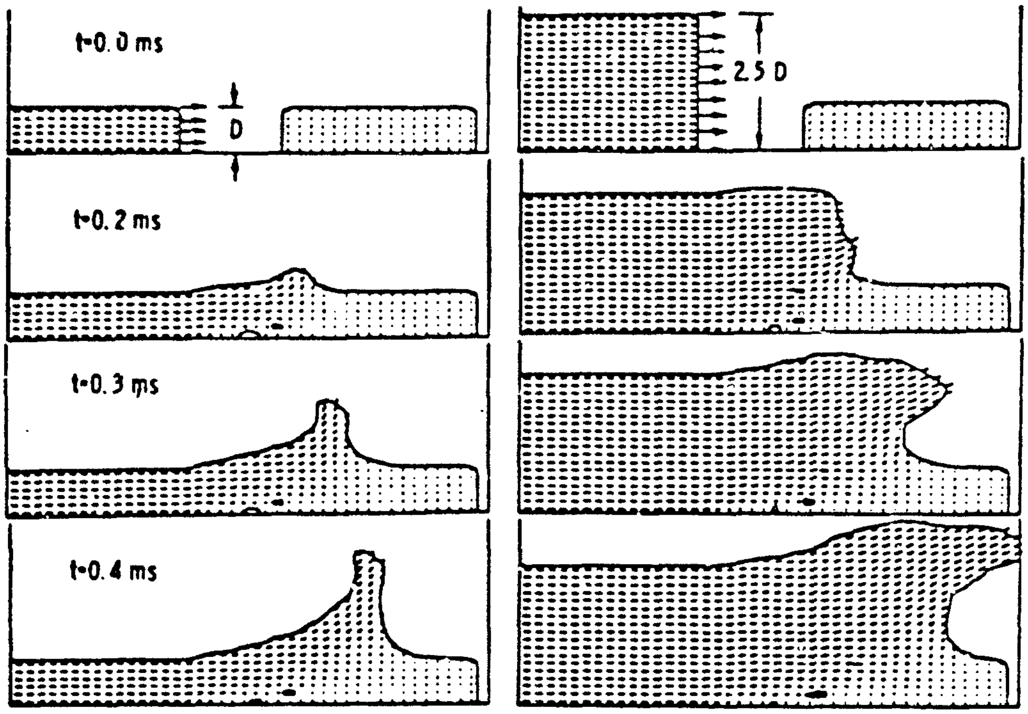

Figure 9. Flow Patterns (One Fluid Flow, $\nu_w = \nu_c = 9.8\ mm^2/s$, $V_j = 10\ m/s$, $\theta = 0°$)

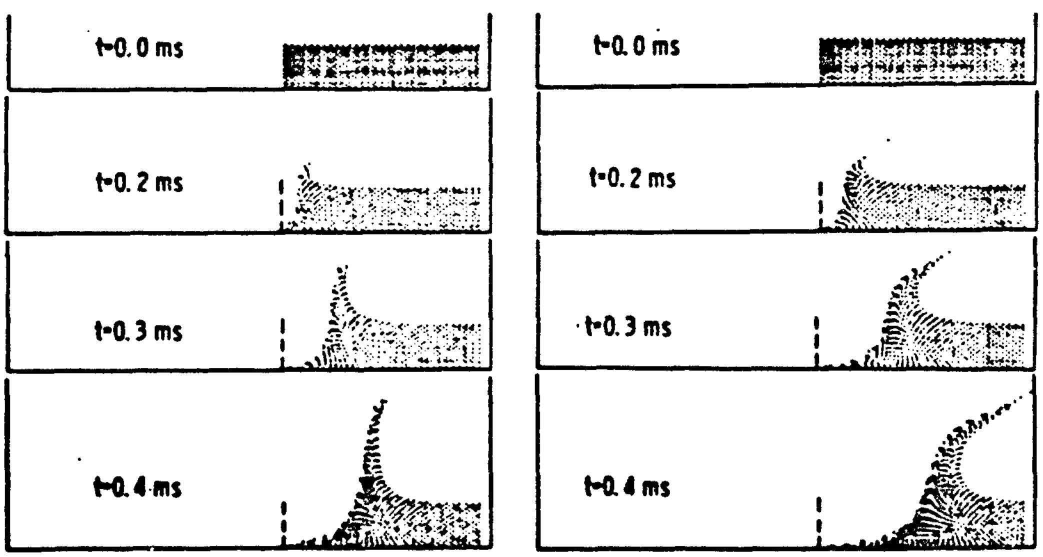

Figure 10. Evolution of Contaminant Droplets (One-Fluid Flow, $\nu_w = \nu_c = 9.8\ mm^2/s$, $V_j = 10\ m/s$, $\theta = 0°$)

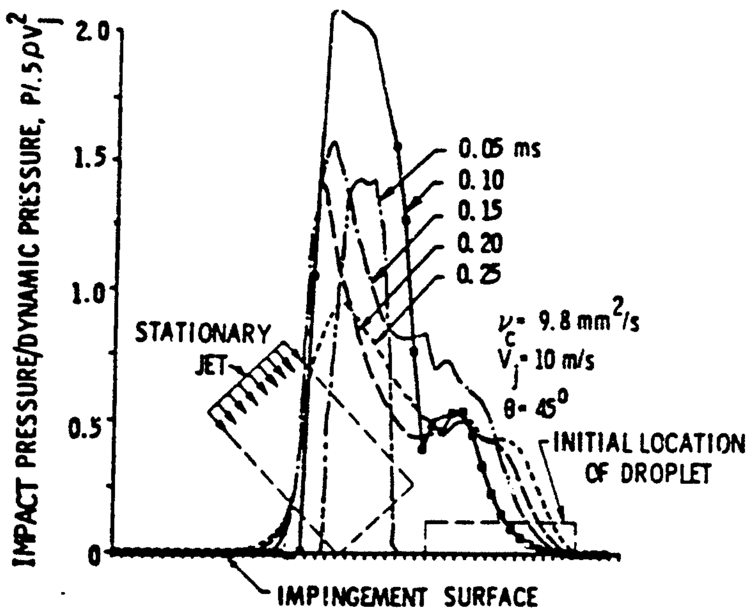

Figure 11. Instantaneous Impact Pressure Distribution on Impingement Surface

IV. CONCLUSIONS

The computer simulation is useful for observing details of the flow development following the commencement of the jet impingement. The results indicate that the contaminant viscosity ν_c, the jet velocity V_j, and the jet incidence angle θ have strong effects on the profile and the displacement of the contaminant droplet. The computer simulation shows that for $V_j = 5$ m/s and $\nu_c = 9.8$ mm^2/s, a jet at an incidence angle of $\theta = 45 \sim 60°$ gives the best performance in displacing the droplet. Because the flow is transient the instantaneous impact pressure on the impingement surface may rise higher than the corresponding steady-state dynamic pressure of the jet. For a limited jet flow rate, an increase in jet velocity rather than jet size will likely give a better decontamination result.

Further studies on surface tension effects, moving jets, and optimization of flow parameters are in progress.

DISTRIBUTION LIST

No. of Copies	Organization
12	Administrative Defense Technical Info Center ATTN: DTIC-DDA Cameron Station Alexandria, VA 22314
1	Commander US Army Materiel Development and Readiness Command ATTN: DRCDMD-ST 5001 Eisenhower Avenue Alexandria, VA 22333
1	Commander US Army Armament Research and Development Command ATTN: DRDAR-TDC Dover, NJ 07801
2	Commander US Army Armament Research and Development Command ATTN: DRDAR-TSS Dover, NJ 07801
1	Commander US Army Armament Material Readiness Command ATTN: DRSAR-LEP-L Rock Island, IL 61299
1	Director US Army Armament Research and Development Command Benet Weapons Laboratory ATTN: DRDAR-LCB-TL Watervliet, NY 12189
1	Commander US Army Aviation Research and Development Command ATTN: DRDAV-E 4300 Goodfellow Blvd St. Louis, MO 63120
1	Director US Army Air Mobility Research and Development Laboratory Ames Research Center Moffett Field, CA 94035

No. of Copies	Organization
1	Commander US Army Communications Rsch and Development Command ATTN: DRSEL-ATDD Fort Monmouth, NJ 07703
1	Commander US Army Electronics Research and Development Command Technical Support Activity ATTN: DELSD-L Fort Monmouth, NJ 07703
1	Commander US Army Missile Command ATTN: DRSMI-R Redstone Arsenal, AL 35898
1	Commander US Army Missile Command ATTN: DRSMI-YDL Redstone Arsenal, AL 35898
1	Commander US Army Tank Automotive Command ATTN: DRSTA-TSL Warren, MI 48090
1	Director US Army TRADOC Systems Analysis Activity ATTN: ATAA-SL White Sands Missile Range NM 88002
2	Commandant US Army Infantry School ATTN: ATSH-CD-CSO-OR Fort Benning, GA 31905
1	AFWL/SUL Kirtland AFB, NM 87117

DISTRIBUTION LIST

No. of Copies	Organization
	Aberdeen Proving Ground
	Dir, USAMSAA ATTN: DRXSY-D DRXSY-MP, H. Cohen
	Cdr, USATECOM ATTN: DRSTE-TO-F
	Dir, USACSL ATTN: DRDAR-CLB-PA DRDAR-CLN DRDAR-CLJ-L DRDAR-CLB-PO (2 cys)

USER EVALUATION OF REPORT

Please take a few minutes to answer the questions below; tear out this sheet, fold as indicated, staple or tape closed, and place in the mail. Your comments will provide us with information for improving future reports.

1. BRL Report Number ______________________________

2. Does this report satisfy a need? (Comment on purpose, related project, or other area of interest for which report will be used.)

____

____

____

3. How, specifically, is the report being used? (Information source, design data or procedure, management procedure, source of ideas, etc.) ______________________________

____

____

4. Has the information in this report led to any quantitative savings as far as man-hours/contract dollars saved, operating costs avoided, efficiencies achieved, etc.? If so, please elaborate.

____

____

5. General Comments (Indicate what you think should be changed to make this report and future reports of this type more responsive to your needs, more usable, improve readability, etc.) ______________

____

____

____

6. If you would like to be contacted by the personnel who prepared this report to raise specific questions or discuss the topic, please fill in the following information.

Name: ______________________________

Telephone Number: ______________________________

Organization Address: ______________________________

____

____